Limitations of Monoolein in Simulating Water-in-Fuel Characteristics of EN590 Diesel containing Biodiesel in Water Separation Testing

Abstract

In modern diesel fuel a proportion of biodiesel is blended with petro-diesel to reduce environmental impacts. However, it can adversely affect the operation of nonwoven coalescing filter media when separating emulsified water from diesel fuel. This can be due to factors such as increasing water content in the fuel, a reduction in interfacial tension (IFT) between the water and diesel, the formation of more stable emulsions, and the generation of smaller water droplets. Standard water/diesel separation test methods such as SAE J1488 and ISO 16332 use monoolein, a universal surface-active agent, to simulate the effects of biodiesel on the fuel properties as part of water separation efficiency studies. However, the extent to which diesel/monoolein and diesel/biodiesel blends are comparable needs to be elucidated if the underlying mechanisms affecting coalescence of very small water droplets in diesel fuel with a low IFT are to be understood.

To address this challenge, test fuels composed of reference diesel (REF diesel)/biodiesel and REF diesel/monoolein were experimentally studied to determine fuel properties such as IFT, water content, and dynamic viscosity, as well as online droplet size distributions with reference to IFT. It was found that biodiesel and monoolein do not influence the IFT of water in fuel in a comparable manner and resulting water droplet size distributions are substantially different. Fuels blended with biodiesel exhibited higher viscosity and water content than fuel freshly blended with monoolein. Online measurement of water droplet sizes revealed substantially smaller water droplets in biodiesel blends compared to monoolien blends at the same IFT measured using offline tensiometry. These results may be instructive for the development of standard test methods that simulate the effect of biodiesel blends in fuel-water separation, as well as for improving the design of fuel-water separation systems.

Keywords: Biodiesel; Monoolein Surfactant, Coalescence; Water separation; Fuel characterization.

1. Introduction

Emission control regulations established by The United States Environmental Protection Agency (EPA) and the council of the European Union, have led to the development of a standard diesel fuel composition known as EN590, as well as high-pressure common-rail (HPCR) injection systems (Figure 1) [1, 2]. The EN590 fuel is composed of Ultra-Low Sulphur Diesel (ULSD), up to 7% of which is composed of biodiesel, and a variety of fuel performance enhancement additives. In HPCR systems, microlitres of fuel are injected in to the engine multiple times during every cycle at a high pressure of about 2500 bar, while the tolerances

for fuel injection have reduced to a micrometre scale [3, 4]. Such a sensitive system requires highly efficient fuel-water separation to ensure water-free fuel is presented to the injection system and serious damage such as wear and corrosion as well as formation of biological sludge and sediments in the fuel lines are avoided [1, 5-12].

Evaluation of the water separation performance of filters depends on their end use, and standards such as SAE J1488 and ISO 16332 define the test conditions required [13, 14]. These laboratory tests are usually conducted using a base reference grade diesel fuel that is free of solid contaminants or biodiesel but is blended with a specified surfactant (surface active agent) such as monoolein, which alters the fuel's interfacial tension (IFT), the water separability of such fuels can also be measured using a sedimentation test (ASTM D1401). The approach is based on the theory that a low IFT will result in small droplet sizes (< 25μm [13]), which should simulate more challenging fuels such as EN590 diesel. Fuel additives in EN590 fuel are known to act as surfactants, which are amphiphilic and able to lower the interfacial tension (IFT) of oil/water emulsion phases resulting in small, stable droplets that are a challenge for water separation.

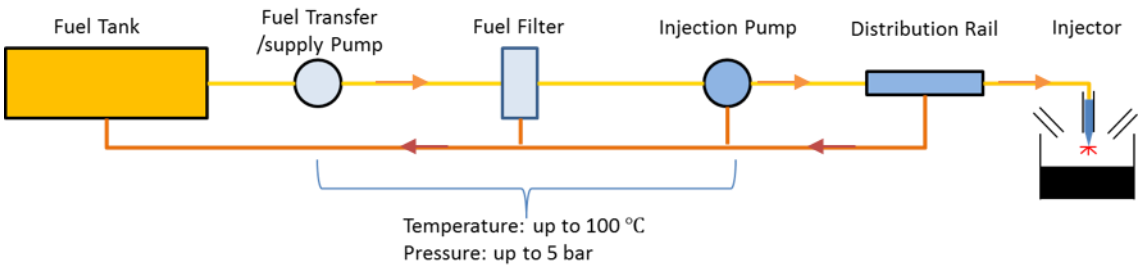

Figure 1 Simple schematic of a high-pressure common rail fuelling (HPCR) system: orange arrows show the fuel feeding direction and red arrows shows return of excess fuel to the tank

A threshold of 200 ppm (v/v) total water in diesel fuel is defined by the EN590 standard as an acceptable level by Original Equipment Manufacturers (OEMs) in Europe and North America [4, 15]. However, in reality the total water level of fuel within the vehicle tank can increase because of condensation as well as the conditions under which the fuel is maintained during storage, transfer, and transport from the refinery to the petrol station. There may also be differences in dissolved water content due to variations in fuel composition resulting from blending biodiesel. Biodiesel is more hygroscopic than petro-diesel and has affinity to water due to the presence of alkyl-esters and the unsaturated molecular structure, such that the water content of the fuel can increase [15-21].

Water in a diesel fuelling system can take three forms: dissolved, free (settled), or emulsified, depending on circumstances [1, 22-25]. In a vehicle fuel tank, where agitation is minimal, water and diesel can form a single interface because the liquids are immiscible, and the interfacial tension (IFT) is measured at the interface surface. The free water is disturbed when it is exposed to the shear stress of the fuel moving through the fuel pump, such that it forms a spherical interface in the form of an emulsified water droplet in the fuel.

The dispersed water is characterised by its droplet size distribution (DSD), which depends on the type and specification of the fuel pump and fluid parameters governing the fluid shear stress, $\tau\ (\mathrm{Pa})$ (Equation 1), which includes the velocity gradient of the fluid layers, $\omega\ (\mathrm{s}^{-1})$ and the dynamic viscosity, $\mu_c\ (\mathrm{Pa.s})$. The water and fuel IFT, $\gamma\ (\mathrm{N/m})$ governing the internal Laplace pressure of the water droplet, $P_l\ (N/m^2)$ is also important, where r is the droplet radius (Equation 2) [24, 26, 27].

$$\tau = \mu_c \times \omega\,, \qquad \omega = \frac{du}{dy}$$

Equation 1 Shear stress in a fluid

$$P_l = \frac{2\gamma}{r}$$

Equation 2 Laplace pressure across the surface of a spherical droplet

The shear stress of the bulk fuel competes with the internal Laplace pressure of the water droplet to rupture it, such that at a given flow rate, the probability of smaller water droplets in the fuel of higher viscosity and lower IFT, increases.

In water-in-fuel emulsions of high internal energy, dispersed droplets tend to collide and coalesce into larger droplets, and this droplet enlargement process continues until a single interface between the two phases is achieved [24, 27-29]. Equation 3 indicates the settling velocity (V) of a droplet with a density of ρ_w and a radius of r, settling down in a bulk fuel with a viscosity of μ and a density of ρ_f, where g is the acceleration due to gravity.

$$V = \frac{2(\rho_w - \rho_f)gr^2}{9\mu}$$

Equation 3 Settling velocity of a water droplet dispersed in fuel

The breakdown of the emulsion requires time, which can be of the order of hours if the emulsion is stabilised by surface active agents in the fuel [1, 22-24, 27, 28, 30]. In real vehicle situations, fuel additives including biodiesel tend to act as surfactants as they are usually

composed of amphiphilic molecules that reduce the water/fuel interfacial tension (IFT) and stabilise small size water droplets in the fuel [1, 7-10, 31-34]. Therefore, the droplets have low settling velocities and also the surfactants can prevent droplet enlargement by inducing resistance to coalescence and the formation of repellent and/or electrostatic barriers between the water droplets.

Petiteaux [4] demonstrated that 20:80 blends of biodiesel/petro-diesel reduce water sedimentation and IFT by 1.5% and 19% respectively, and that B20 (blend of 20% biodiesel in petro-diesel v/v) fuel can possess a saturation level more than twice that of petro-diesel. Other studies [13, 15, 35] found that the IFT and water separation behaviour of blends containing more than 20% biodiesel are very similar to pure biodiesel (B100), and the change in both parameters does not hold as the proportion of biodiesel increases up to B100. However, a thorough search of the relevant literature yielded no consistent explanation for this behaviour. Tang [15] claimed that the fuel viscosity can almost double if biodiesel is blended with petro-diesel, which can be beneficial for capturing small, solid particles, e.g. <20μm. However, the addition of biodiesel can reduce water separation efficiency owing to the influence of biodiesel on IFT. It has also been reported that the total water content of diesel measured in the tank of a vehicle can be as high as 5000 (v/v) ppm [4, 26], and pure biodiesel (B100) can have a water saturation content of ≥1300 ppm [13, 15, 35]. Moreover, Yoshino et al. [13] using the ISO 16332 test stand methodology, claimed that the addition of just 5% biodiesel (B5) can reduce water separation efficiency in the fuel from 95% to 85% due to a decrease in the fuel IFT (22.9 mN/m to 12.9 mN/m) as well as increase the separation time (13s to 150s - according to the sedimentation test, ASTM D 1401).

The presence of surfactants also influences water separation from diesel. Petiteaux [4] and Schutz [34] reported that water separation from ULSD fuel is more challenging than Low Sulphur diesel due to the presence of additives that modify lubricity, cetane number, and the level of deposits in ULSD fuel. They also suggested that in the presence of surfactants, a decrease in IFT is time-dependent due to the dynamic movement of surfactant molecules from the bulk fluid to the water/fuel interface. Moreover, a study of different types of surfactant revealed no absolute correlation between associated changes in IFT and that of water separation (sedimentation of water droplets) [4, 34]. This is in agreement with the results of Pangestu [1], which suggested that droplet size and its persistence in an emulsion is not only driven by IFT, but also by the ability of the surfactant to stabilise dispersed droplets from coalescence.

Although the impact of biodiesel and surfactants on water-in-fuel emulsion properties and water separation has been previously investigated, comparative data on water droplet size distributions and water separation performance associated with blends of diesel/biodiesel and diesel/monoolein is lacking. The extent to which biodiesel/petro-diesel blends and

surfactant/petro-diesel blends can be compared in terms of water/diesel IFT and water droplet size distribution in fuel is crucial to understand their roles in water separation. Such understanding is needed to underpin development of improved coalescing filter media that are less sensitive to fuel composition as well as to inform the development of new standard test methods. Accordingly, the aim of this work was to investigate the emulsion properties and water droplet size distribution (DSD) characteristics of Rapeseed oil Methyl Ester (RME) biodiesel and the surfactant monoolein (Sigma® 1-Oleoyl-rac-glycerol) when blended in petro-diesel fuel. Monoolein (Sigma® 1-Oleoyl-rac-glycerol) was selected in light of its recommended application in the SAE 1488 and ISO 16332 standard test procedures. The interfacial tension, fuel water content, dynamic viscosity, and density of the fuel were also elucidated using standard test procedures.

2. Experimental methods

2.1. Preparation of test fuel blends

Biodiesel blends were prepared by mixing pure rapeseed oil methyl ester (RME) biodiesel (B100, Carcal B100 RME (Off-road) - Petrochem Carless Limited, UK), into an additive-free reference grade diesel (REF) (CEC RF-06-03 diesel - Hess Corporation, Germany). Biodiesel oxidation levels were not measured, but all fuels for testing were extracted from unopened barrels. Diesel fuel blends were designated as Bi where i = the volume fraction of biodiesel (v/v) x 100%. B5 therefore consists of a blend of REF and 5% biodiesel. The petro-diesel and surfactant blends were prepared by mixing a specified volume (ppm) of monoolein ((1-(cis-9-Octadecenoyl)-rac-glycerol, density of 969 kg/m3), Sigma Aldrich UK) in the reference grade diesel (Mi), where i = the volume fraction of monoolein (v/v) x 1000000. M200 therefore refers to a blend of REF with 200 ppm monoolein (v/v).

2.2. Fuel characterisation

The characterisation methods and test fuels used for each method are summarised in Table 1.

Table 1: Fuel properties and their standard test procedures

Property	Unit	Test fuels	Standard No.	Test Temperature (℃)
Water content	$ppm\ (v/v)$	REF, B5, B10, B15, B20, B30, B50, B100 M200, M3625, M400, M600, M1000	ISO 760:1978	22-25
Interfacial tension	mN/m	REF, B5, B10, B15, B20, B30, B50, B100 M200, M3625, M400, M600, M1000	ISO 6889:1986	22-25
Density	kg/m^3	REF, B5, B10, B15, B20, B50, B100 M400, M1000	ISO 3838:2004	22
Dynamic viscosity	$mPa.s$	REF, B5, B20, B50, B100 M400, M1000	ISO 3104:1996	25

Water content was measured using a coulometer (Metter-Toledo-C20 Compact Karl Fischer) and the IFT was determined using the Wilhelmy plate method via tensiometry (Kruss K20 Easy Dyne force) based on five replicates per sample. The fuel densities were measured using a 25 ml capillary-stoppered pycnometer, with two replicates per sample. The dynamic viscosity ($\mathrm{mPa.s}$) of the test fuels was calculated according to ISO 3104:1996, based on measurement of the Kinematic viscosity ($\mathrm{mm^2/s}$) and density. Kinematic viscosity was measured using a BTI® viscometer (BS/U-tube, size B) for the REF, monoolein blends and B5. A Technico® viscometer (BS/IP/SL size 1) was used to measure fuels containing blends of more than 20% biodiesel (B20). According to the ISO 3105 standard, at least two measurements were performed for each test sample to enable an average of the flow time to be calculated.

2.3. Water separation via the sedimentation test

The sedimentation test used to determine resistance to coalescence modulated by biodiesel and monoolein content in the test fuels followed the ASTM D1401-12E1 test procedure with small modifications. Herein, 40ml of REF, B5, B20, B50, M200, and M325 was separately mixed with 10 ml distilled water in a measuring cylinder for 30 s at 1000-12500 r $\mathrm{min^{-1}}$ using a MICROSEP® emulsifier (ASTM D7261 – 13) at room temperature. After emulsification, the fuel blends were compared semi-quantitatively by recording the volume of the coalesced water versus time for the test fuels. More time is required to recover the total volume of water if the water-in-fuel is stable, there is more resistance to coalescence in the emulsion, and water droplets exhibit low settling velocity.

B5 and M200, and B20 and M325, were directly compared due to the similarity in their respective IFTs, i.e. about 18 mN/m and 12 mN/m respectively, and B50 was used to

consider the effect of viscosity on the water separation as it has the same IFT as B20 but higher viscosity than other fuel blends. REF fuel was used as the control sample.

2.4. Water Droplet size distribution (DSD)

An emulsion generation test rig equipped with an online droplet size measurement system (Insitec Malvern® particle size analyser) was employed to characterise water droplet size distribution in the test fuels. The in-house built rig emulsifies 0.2% (v/v) Deionised water in a test fuel and measures droplet size distribution at both atmospheric and four bar static pressures. A schematic of the test rig is shown in Figure 2. The rig consists of one circuit enabling a single-pass test through a particle sizer for analysis of droplet size distribution. The Parker Nicholas pump (Heavy Duty Engine Platform Gerotor, 5000 r min^{-1}, 24V~7 l /min @ 6 bar) (P) circulates at least 10 l of a fresh test fuel from the reservoir (F2) at a flow rate of ~ 6 l/m, through the particle size analyser (M), flowmeter (FM), and high efficiency Parker Racor Dmax® clean-up filters (CF). Deionised water reserved in the tank (W) at the suction side of the main pump (P) is injected into the system by opening the valve (V) via pump suction or based on the hydrostatic pressure in the tank. Once injection is started, fuel is collected in the storage reservoir (F1) instead of tank F2 to provide a single pass emulsion test. The injection rate was constant at 12 ml/min during a water injection experiment of 1 min. To run a test at the higher pressure, the pressure valve (PV) was adjusted to reach 4 bar static pressure using the same procedure.

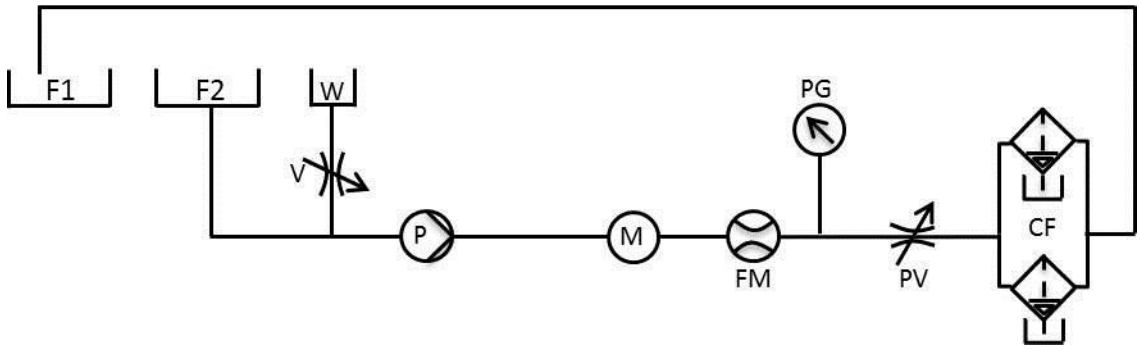

Figure 2. Schematic of the emulsion generation test rig

Water droplet sizes were measured over a range of 0.1$\mu\mathrm{m}$ to 2500 $\mu\mathrm{m}$ during injection using laser diffraction at a wavelength of 670nm. The received data from thirty-two detectors for the angular variation in intensity of light scattered by dispersed water droplets is interpreted to calculate their diameter. The REF, B5, B10, B20, B30, B50, B100, M200, M400, M600, and M1000 fuel compositions were evaluated. The output was an average distribution for a volume equivalent spherical diameter of the water droplets of the emulsion during the water injection. For each emulsion, a volume median diameter, denoted as Dv_{50}, was also calculated from

their cumulative distribution curves. Figure 3 gives an example of the average water droplet size distribution in the REF fuel. The refractive indices of the fuel blends needed to calculate the droplet size distributions was obtained via a CETI® Abbe refractometer.

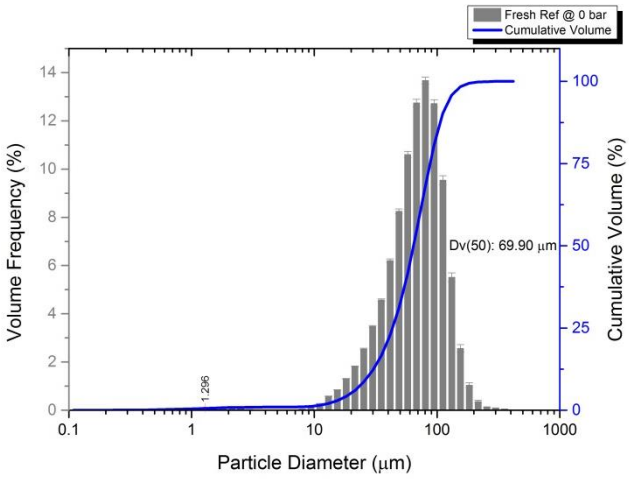

Figure 3. Example of an in-line water droplet size distribution during injection for the reference diesel

3. Results and discussions

3.1. Fuel characterisation

The biodiesel and monoolein blends were of dissimilar density (kg/m^3), dynamic viscosity ($mPa.s$), IFT ($mN/m \pm SE$), and water content ($ppm(\frac{v}{v}) \pm \mathrm{SE}$), as illustrated in Figure 4 to Figure 7 respectively.

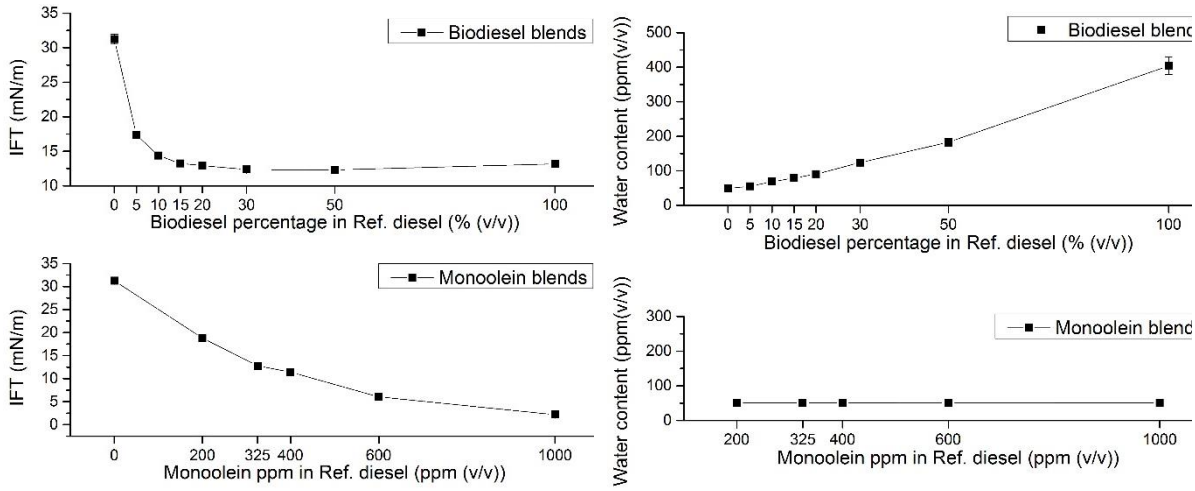

Figure 4. IFT of the biodiesel and monoolein blends

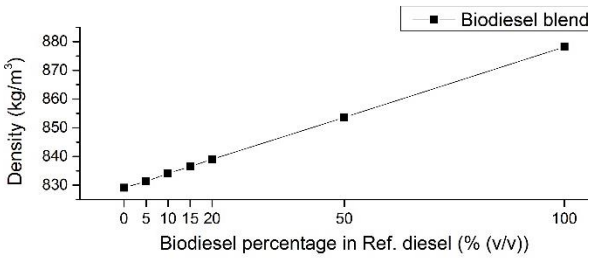

Figure 5. Water content of the biodiesel and monoolein blends

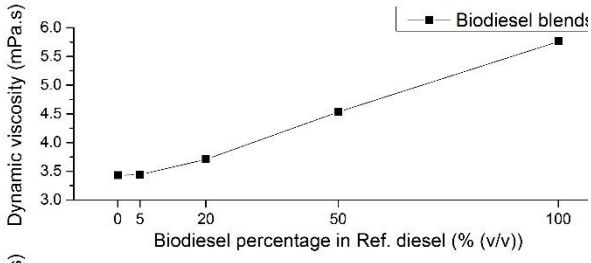

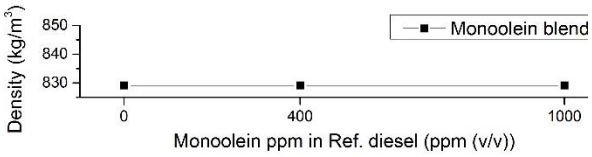

Figure 6. Density of the biodiesel and monoolein blends

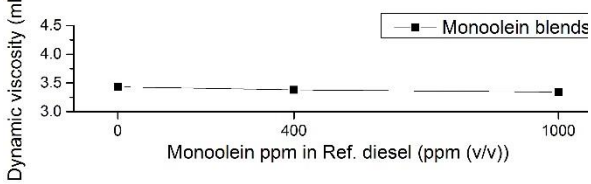

Figure 7. Dynamic viscosity of the biodiesel and monoolein blends

Figure 4 confirmed that biodiesel acts as a surface-active agent such that the IFT of the REF fuel reduced from 31.24±0.73 $\mathrm{mN/m}$ to 13.17±013 $\mathrm{mN/m}$ in B100. This is in agreement with findings in the literature [13, 15, 35]. However, it is noteworthy that the trends in the IFT data for the fuels containing biodiesel and monoolein are not the same when the blend proportions increase to B100 and M1000 respectively.

As the biodiesel content increases from B20 to B100, the IFT does not continue to decrease, i.e. the IFT remains almost constant at about 12 $\mathrm{mN/m}$ for B20, B30, B50, and B100. However, further decreases in IFT are observed as the monoolein content increases. This can be attributed to the capability of the water and fuel interface to accommodate monoolein molecules at a concentration of 1000 ppm while the interface is not being saturated by them. As a result, the IFT decreases by adding more monoolein, (IFT of 2.18 ± 0.12 $\mathrm{mN/m}$) for M1000 (Figure 8). This is in contrast to the biodiesel blends containing more than 20% biodiesel in which the interface reaches its saturation point and the behaviour of the interface is dominated by the chemistry of the biodiesel (Figure 9). This can be explained by comparing the molar ratios of the biodiesel and monoolein blends. For instance, the molar concentrations of B20 and M325, which exhibited identical IFTs, were 0.5924 and 0.0009 mol/l respectively (molecular weight of monoolein (C21H40O4) = 356.54 g/mol. Note that methyl oleate (C19H36O2) has a molecular weight of 296.494 g/mol and is a typical biodiesel fuel [36]). Thus, a lower number of monoolein molecules are available to saturate the fuel-water interface, as compared to biodiesel molecules, in each of the fuel blends.

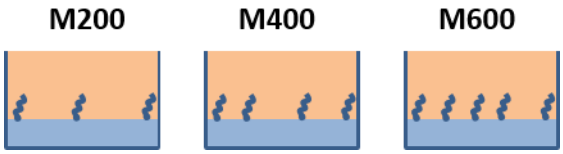

Figure 8:Schematic of the interface of water and monoolein blends

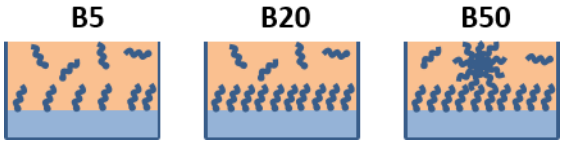

Figure 9: Schematic of the interface of water and biodiesel blends

The water content measurements (Figure 5) reflect the fact that biodiesel has more affinity for water than petro-diesel. For example, water contents of 49.13±2.79 $ppm\ (v/v)$ and 403.94±24.89 $ppm\ (v/v)$ were measured for the REF and B100 fuels respectively, which is in agreement with the findings in the literature [15-21, 37, 38]. This is due to the higher polarity of the biodiesel molecules (alkyl-esters and unsaturated molecular structure) compared to that of petro-diesel. However, it is interesting to note that as the proportion of monoolein increases from zero (REF) up to 1000 ppm (M1000), changes in in the water content of the fuel are not noticeable. This is also likely to be attributed to a lower molar ratio of monoolein compared to that of biodiesel in the test fuels, which results in a lower overall hygroscopicity of the monoolein blends.

According to Figure 6, it was found that a fuel blend containing a higher proportion of biodiesel exhibits a higher density compared to the reference diesel. This is because the biodiesel (B100) has a higher intrinsic density (878.2 kg/m^3) and water content (403.94±24.89 $ppm\ (\frac{v}{v})$) compared to the REF fuel with a density and water content of 829.1 kg/m^3 and 49.13±2.79 $ppm\ (\frac{v}{v})$ respectively, which affects the density of the biodiesel blends. By contrast, there was no marked change in the density of the monoolein blends resulting from the addition of monoolein up to 1000 ppm in the REF diesel.

The biodiesel blends exhibited higher viscosities than the REF fuel (Figure 7), e.g. 5.76 $mPa.s$ in B100 and 3.43 $mPa.s$ in REF fuel. On the other hand, no variation was observed in the fuel viscosity of the monoolein blends, which is likely to be connected with the low molar ratio of the monoolein compared to the biodiesel in the test fuels.

3.1. Water separation via the sedimentation test

Table 2 summarises the volume of settled water at different time intervals in each of the fuel samples, and Table 3 demonstrates the appearance of the samples at the 3rd minutes of the test.

Table 2. Water separation (settlement) in the test fuels (ml)

Time (min) / Fuel	1	2	3	4	5	6	7	8	9
REF	8	10	10	10	10	10	10	10	10
B5	4	9	10	10	10	10	10	10	10
B20	-	-	7	7	7-8	8	8-9	9	10
B50	-	-	7	8	9	9	10	10	10
M200	8	11	10	10	10	10	10	10	10
M325	-	5-7	7-9	7-9	10	10	10	10	10

Table 3. Visual assessment of water separation in fuel blends

	REF	B5	B20	B50	M200	M325
3rd min						

It was apparent that the biodiesel blends produced longer settling times compared to the monoolein blends and the REF fuel, and water droplets were more stable in B20 and B50 compared to the other test fuels. This could be the result of the higher viscosity of the biodiesel blends as well as their ability to stabilise water droplets of smaller size resulting in a reduction in the settling velocity of the dispersed water.

Visual assessment of the REF mixture revealed settled water that first appeared milky in colour but which gradually cleared. However, in the fuels containing biodiesel and monoolein, progression from the milky phase to clear water was accompanied by a flocculation phase containing water. This was indicative of a resistance to coalescence associated with the presence of the surfactant or biodiesel molecules at the interface of the water droplets. Comparing the fuel phases in each of the samples, B50 appeared clearer than the other

blended fuels, which may be attributable to the relatively high capability of B50 to dissolve small water droplets.

3.2. Water droplet size distribution

The Dv_{50}s of water droplets (mean$\pm SE$) at atmospheric and 4 bar pressures in the test fuels are listed in Table 4. The required refractive indexes of the blends for plotting the size distributions were measured as 1.454 and 1.458 for B100 and B50 respectively, and the same value of 1.461 for the other fuel blends.

Based on Table 4, Dv_{50} of the REF fuel decreased from 69.9 ± 0.23 μm to 34.4 ± 0.07 μm by addition of 50% biodiesel (B50) and reduced to 46.78 ± 0.13 μm by addition of 1000 ppm monoolein (M1000). This data confirms that both monoolein and biodiesel reduce water droplet size in the fuel and are able to stabilise water droplets at a lower size compared to the reference grade diesel at an identical flow rate. Moreover, comparing Dv_{50}s at different pressures shows that by increasing the static pressure during emulsion generation to 4 bar, smaller droplet sizes were formed compared to atmospheric pressure. This reduction was observed for all the test fuels. This is of practical significance because in diesel fuel engines, high pressures are increasingly used, meaning smaller droplet sizes are likely to be increasingly encountered.

Table 4: Dv_{50} (μm) of dispersed water droplets in monoolein and biodiesel blends at atmospheric and 4 bar pressures

Test Fuel	Atm. pressure	4 bar pressure	Test Fuel	Atm. pressure	4 bar pressure
REF	69.9 ± 0.23	66.27 ± 0.6	**M200**	62.28 ± 0.18	58.95 ± 0.21
B5	49.81 ± 0.1	-	**M400**	57.19 ± 0.17	54.77 ± 0.19
B10	44.07 ± 0.08	41.21 ± 0.09	**M600**	54.74 ± 0.35	-
B20	40.13 ± 0.06	38.03 ± 0.07	**M1000**	46.78 ± 0.13	-
B30	35.38 ± 0.05	33.79 ± 0.05			
B50	34.4 ± 0.07	31.78 ± 0.05			
B100	32.81 ± 0.06	31.54 ± 0.05			

To characterise monoolein and biodiesel regarding the water droplet size, the Dv_{50} of water droplets in the fuel blends at atmospheric pressure were plotted with regard to the IFT of the test fuels as shown in the Figure 10.

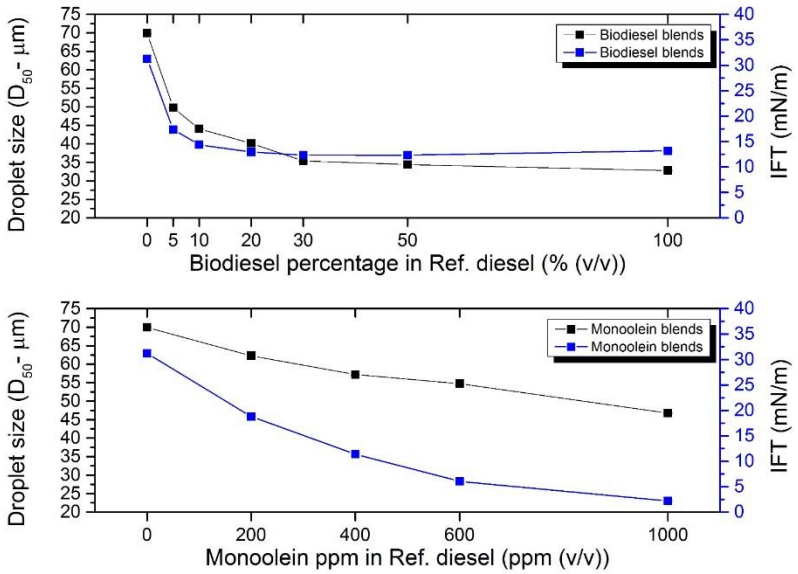

Figure 10. *Dv50* for dispersed water droplets at atmospheric pressure, related to the IFT of the monoolein and biodiesel blends

Based on Figure 10, at an IFT between 17 and 19 mN/m, the Dv_{50} of water droplets in B5 was much smaller than that measured for M200 (49.81 ± 0.1 µm Vs. 62.28 ± 0.18 µm). The Dv_{50} of the water droplets in B20 was also smaller than that of M400 at an IFT over a range of 11 - 13 mN/m. This indicates that the biodiesel blends exhibited smaller Dv_{50} values compared to the monoolein blends at corresponding IFT values. Regardless of the chemical composition of the monoolein and biodiesel molecules, this can be attributed to the lower molar ratio of the monoolein than the biodiesel in the fuel blends, e.g. 0.5924 and 0.0009 mol/l in B20 and M325 respectively, resulting in an inability of monoolein to maintain the IFT in the emulsion as low as was measured via tensiometry.

During an IFT measurement via tensiometry, the IFT of the interface between the fuel and water phases is measured while the linear interface is stable and has a constant surface area during the measurement. However, when the same volume of water is emulsified in the fuel, the surface area of the fuel-water interface increases, which is because of water droplets dispersed in the fuel. Therefore, a greater number of surfactant molecule is required to maintain the IFT of the emulsion at the same value as what is measured via tensiometry. In the case of the monoolein and biodiesel, there are a greater number of biodiesel molecules in the biodiesel blends compared to the number of monoolein molecules (Figure 11) such that the biodiesel blends provide many more surfactant molecules compared to the monoolein blends enabling the fuels to stabilize the emulsified droplets at a smaller size.

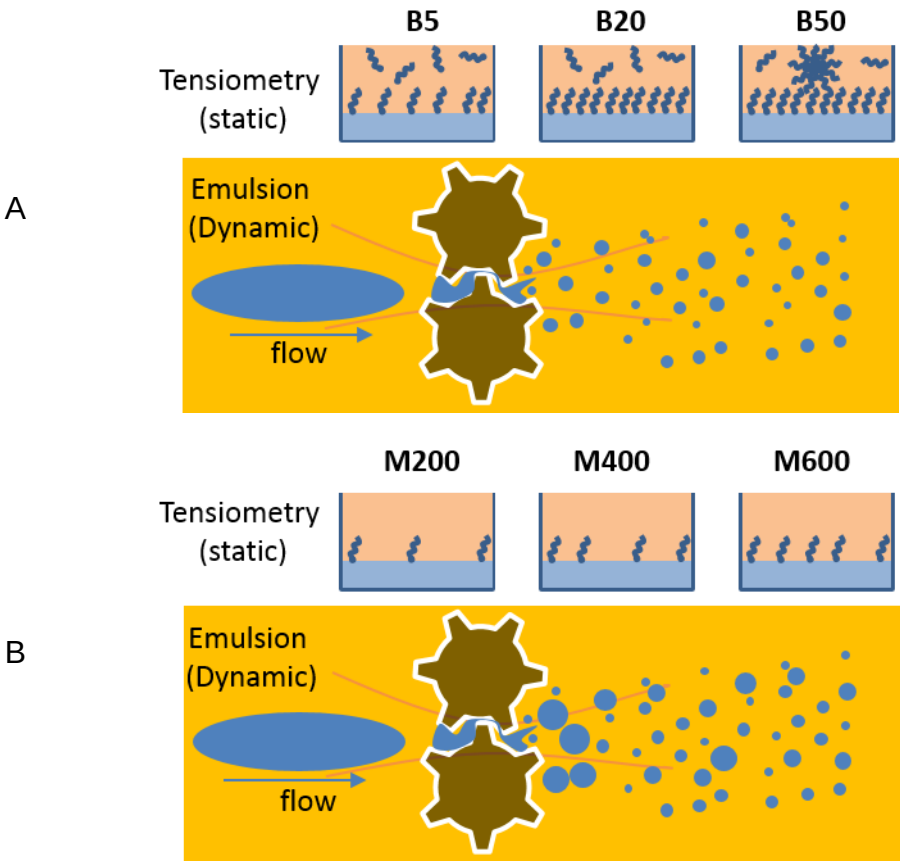

Figure 11: Effects of molar concentration of A) biodiesel and B) monoolein in changing fuel-water interface characteristics in static and dynamic conditions

Based on this and also the fact that the biodiesel blends had a higher viscosity than the monoolein blends at an identical IFT, water droplets are exposed to a greater shear stress competing with their lower Laplace pressure in the biodiesel blends compared to the monoolein blends, which could contribute to the formation of smaller droplets in biodiesel blends.

4. Conclusion

In this work, the effects of biodiesel and monoolein on the behaviour of diesel fuel in terms of interfacial tension (IFT), dissolved water content and viscosity were considered, and the resultant impact on water-in-fuel emulsions was further explored with reference to biodiesel and monoolein surfactant. Following construction of a bespoke emulsion generation test rig, online measurements of water droplet size distributions in diesel containing biodiesel and monoolein were undertaken, and water separation was also evaluated using sedimentation tests.

In existing test standards, specifically ISO 16332 and SAE J1488, monoolein surfactant is employed to adjust the IFT of the reference grade test fuel so as to mimic the presence of fuel

additives including biodiesel in petrol station diesel. However, the results reported herein, raise questions about the suitability of monoolein as an appropriate fuel additive for the test standard, because it does not behave comparably with biodiesel. Fuel containing biodiesel contained more dissolved water and led to higher viscosities compared to the REF fuel and monoolein blends. This occurs even though biodiesel acts like monoolein as a surface-active agent, reducing the fuel IFT and stabilising water droplets in the fuel such that flocculation occurs during water settlement. It is apparent that biodiesel blends and emulsions are capable of maintaining a low IFT measured by tensiometry. However, this does not happen for monoolein blends due to differences in the molar ratios. This coupled with the higher viscosity in a biodiesel blend leads to smaller water droplet sizes compared to monoolein blends. The effect of the static pressure on DSD was tested by applying 4 bar pressure on the fuel blends in the emulsion rig, revealing that higher pressures lead to a decrease in the droplet size of the emulsion, which is independent of the type of additive (biodiesel or monoolein).

Based on the experimental data reported herein, evaluating the droplet size distribution of an emulsion is thought to be a more useful measure to control surfactant levels in fuel blends rather than water sedimentation, and IFT measurements.

Acknowledgement

This work was financially supported by Parker Hannifin Manufacturing (UK).

References

1. Pangestu, F.D. and C.M. Stanfel, *Media for Water Separation from Biodiesel-Ultra Low Sulfur Diesel Blends.* SAE International Journal of Fuels and Lubricants, 2009. **2**(1): p. 305-316.
2. (BSI), B.S.I., *BS EN 590:2013- Automotive fuels - Diesel - Requirements and test methods*. 2013, British Standards Institution (BSI).
3. Johnson, T.V., *Review of Diesel Emissions and Control.* 2010.
4. Petiteaux, M. and G. Monsallier, *Impacts of Biodiesel Blends on Fuel Filters Functions, Laboratory and Field Tests Results*. 2009, SAE Technical Paper.
5. Asmus, A.F. and B.F. Wellington, *Diesel engines and fuel systems*. 1995.
6. Gilles, T., *Automotive Engines: Diagnosis, Repair, Rebuilding*. 2014: Cengage Learning.
7. Shields, C., *High efficiency fuel filter*. 2006, Google Patents.
8. Stone, W., G. Bessee, and C. Stanfel, *Diesel Fuel/Water Separation Test Methods—Where We Are and Where We Are Going.* SAE International Journal of Fuels and Lubricants, 2009. **2**(1): p. 317-323.
9. Shields, C. *Chemical and Thermal Stability of Nonwoven Filtration Media In Fluid Power Applications NCFP I05-19.2*. in *Proceedings of the national conference on fluid power*. 2005.
10. Shields, C. *Design and Performance of Diesel Fuel Filters*. 2005.
11. Association, A.W.W., *Internal Corrosion of Water Distribution Systems, 2 Edition*. 1996: American Water Works Association.
12. EPA, u.s.e.p.a. *Air Emissions*. 2014 [cited 2014 5/22/2014].
13. Yoshino, F.J., G.A. Marques, and F. Ferrari, *Water Separation Challenge for Brazilian Diesel Engine*. 2013, SAE Technical Paper.
14. Lopes, S.M. and T. Cushing, *The Influence of Biodiesel Fuel Quality on Modern Diesel Vehicle Performance*. 2012, SAE Technical Paper.
15. Tang, T.-W., Y.-Y. Ku, and C.L. Chen, *Impacts of Biodiesel Blends on Fuel Filters of High Pressure Common Rail (HPCR) System*. 2016, SAE Technical Paper.
16. Knothe, G., *Biodiesel and renewable diesel: a comparison.* Progress in Energy and Combustion Science, 2010. **36**(3): p. 364-373.
17. Timilsina, G.R. and A. Shrestha, *How much hope should we have for biofuels?* Energy, 2011. **36**(4): p. 2055-2069.
18. Aatola, H., et al., *Hydrotreated vegetable oil (HVO) as a renewable diesel fuel: trade-off between NOx, particulate emission, and fuel consumption of a heavy duty engine.* SAE paper, 2008(2008-01): p. 2500.
19. Atadashi, I., M. Aroua, and A.A. Aziz, *Biodiesel separation and purification: a review.* Renewable Energy, 2011. **36**(2): p. 437-443.
20. Atabani, A.E., et al., *A comprehensive review on biodiesel as an alternative energy resource and its characteristics.* Renewable and sustainable energy reviews, 2012. **16**(4): p. 2070-2093.
21. Basha, S.A., K.R. Gopal, and S. Jebaraj, *A review on biodiesel production, combustion, emissions and performance.* Renewable and Sustainable Energy Reviews, 2009. **13**(6): p. 1628-1634.
22. Stanfel, C. and F. Cousart, *Coalescence media for separation of water-hydrocarbon emulsions*. 2008, US Patents 2009/0178970.

23. Liao, Y. and D. Lucas, *A literature review on mechanisms and models for the coalescence process of fluid particles.* Chemical Engineering Science, 2010. **65**(10): p. 2851-2864.
24. Walstra, P., *Principles of emulsion formation.* Chemical Engineering Science, 1993. **48**(2): p. 333-349.
25. Patel, S.U. and G.G. Chase, *Separation of water droplets from water-in-diesel dispersion using superhydrophobic polypropylene fibrous membranes.* Separation and Purification Technology, 2014. **126**(0): p. 62-68.
26. Stone, W., G. Bessee, and C. Stanfel, *Diesel Fuel/Water Separation Test Methods—Where We Are and Where We Are Going.* SAE International Journal of Fuels and Lubricants, 2009. **2**(2009-01-0875): p. 317-323.
27. Kocherginsky, N.M., C.L. Tan, and W.F. Lu, *Demulsification of water-in-oil emulsions via filtration through a hydrophilic polymer membrane.* Journal of Membrane Science, 2003. **220**(1–2): p. 117-128.
28. He, Y., et al., *Experimental study of drop-interface coalescence in the presence of polymer stabilisers.* Colloids and Surfaces A: Physicochemical and Engineering Aspects, 2002. **207**(1–3): p. 89-104.
29. Christov, N.C., et al., *Capillary mechanisms in membrane emulsification: oil-in-water emulsions stabilized by Tween 20 and milk proteins.* Colloids and Surfaces A: Physicochemical and Engineering Aspects, 2002. **209**(1): p. 83-104.
30. Lehr, F., M. Millies, and D. Mewes, *Bubble-Size distributions and flow fields in bubble columns.* AIChE Journal, 2002. **48**(11): p. 2426-2443.
31. Brown, R. and T. Wines, *Improve suspended water removal from fuels.* Hydrocarbon Processing, 1993. **72**: p. 95-95.
32. (ISO), I.O.f.S., *ISO/TS 16332:2006: Diesel engines -- Fuel filters -- Method for evaluating fuel/water separation efficiency*. 2006.
33. Moorthy, K., *Effect of surface energy of fibers on coalescence filtration*. 2007, University of Akron.
34. Schütz, S., et al., *Water/Diesel Separation. Part 2: Impact of Fuel Additives on the Physical Properties of Water/Diesel Emulsions.*
35. Yoshino, F.J., et al., *Double stage pre-filter diesel water separator.* Blucher Engineering Proceedings, 2015. **2**(1): p. 199-207.
36. Golovitchev, V. and J. Yang. *The Construction of Combustion Models for RME Bio-diesel fuel for ICE Application*. in *ICBT-2008*. 2008.
37. He, B., et al., *Moisture absorption in biodiesel and its petro-diesel blends.* Applied engineering in agriculture, 2007. **23**(1): p. 71-76.
38. Fregolente, P.B.L., L.V. Fregolente, and M.R. Wolf Maciel, *Water content in biodiesel, diesel, and biodiesel–diesel blends.* Journal of Chemical & Engineering Data, 2012. **57**(6): p. 1817-1821.